NeuroImage: Clinical 4 (2014) 623–634

Contents lists available at ScienceDirect

NeuroImage: Clinical

journal homepage: www.elsevier.com/locate/ynicl

Striatal disorders dissociate mechanisms of enhanced and impaired response selection — Evidence from cognitive neurophysiology and computational modelling

Christian Beste[a,†,*], Mark Humphries[b,†], Carsten Saft[c,†]

[a] Cognitive Neurophysiology, Department of Child and Adolescent Psychiatry and Psychotherapy, Faculty of Medicine of the TU Dresden, Germany
[b] Faculty of Life Sciences, University of Manchester, Manchester, UK
[c] Department of Neurology, St. Josef Hospital, Ruhr-University, Bochum, Germany

ARTICLE INFO

Article history:
Received 9 March 2014
Received in revised form 7 April 2014
Accepted 7 April 2014

Keywords:
Computational modelling
Basal ganglia
Executive control
Benign hereditary chorea
Huntington's disease
EEG

ABSTRACT

Paradoxically enhanced cognitive processes in neurological disorders provide vital clues to understanding neural function. However, what determines whether the neurological damage is impairing or enhancing is unclear. Here we use the performance of patients with two disorders of the striatum to dissociate mechanisms underlying cognitive enhancement and impairment resulting from damage to the same system. In a two-choice decision task, Huntington's disease patients were faster and less error prone than controls, yet a patient with the rare condition of benign hereditary chorea (BHC) was both slower and more error prone. EEG recordings confirmed significant differences in neural processing between the groups. Analysis of a computational model revealed that the common loss of connectivity between striatal neurons in BHC and Huntington's disease impairs response selection, but the increased sensitivity of NMDA receptors in Huntington's disease potentially enhances response selection. Crucially the model shows that there is a critical threshold for increased sensitivity: below that threshold, impaired response selection results. Our data and model thus predict that specific striatal malfunctions can contribute to either impaired or enhanced selection, and provide clues to solving the paradox of how Huntington's disease can lead to both impaired and enhanced cognitive processes.

1. Introduction

Paradoxically enhanced cognitive processes in neurological disorders both present stern challenges to our understanding of their underlying mechanisms and provide vital clues to furthering that understanding (Frank et al., 2004; Shiner et al., 2012; Kapur et al., 2013). A key challenge is to solve the underlying paradox of how damage to the same neural system can result in both enhanced and impaired cognitive processes. We took a novel approach to tackling this challenge by using the same cognitive task in two neurological disorders affecting the same system to dissociate their separate functional implications; we then used computational analyses to test the inferred hypothetical effects on the neural system.

We previously showed that Huntington's disease patients have a paradoxical enhancement in a simple auditory decision-making task (Beste et al., 2008; Saft et al., 2008): on trials with irrelevant sensory information, a significantly enhanced mismatch negativity (MMN) signal from EEG recordings corresponded to significantly reduced errors and response times compared to controls. The MMN is defined as a phasic negativity of the event-related potential (ERP) of the EEG evoked by rare deviant stimuli in a sequence of stimuli and may reflect the recognition of rare events deviating from frequent background events by the auditory system (Kujala et al., 2007; Näätänen et al., 2012).

As Huntington's disease primarily affects the striatum, we hypothesized that such paradoxical enhancement of response selection is the result of the interaction between two factors in Huntington's disease progression (Beste et al., 2008): (i) increased NMDA receptor sensitivity at corticostriatal synapses (Fan and Raymond, 2007) and (ii) the consequent degeneration of medium spiny neurons through excitotoxicity, potentially driven by the increased calcium influx through the NMDA receptors. Yet, how or even if this interaction leads to an enhancement of striatal processing is unknown; and even if it does,

Abbreviations: AMPA, α-amino-3-hydroxy-5-methyl-4-isoxazolepropionic acid; BHC, benign hereditary chorea; EEG, electroencephalography; ERP, event related potential; GABA, γ-aminobutyric acid; MMN, mismatch negativity; NMDA, N-methyl-D-aspartate; RON, reorientation of attention; MSN, medium spiny neuron; FSIs, fast spiking interneurons; MMSE, Mini Mental Status Examination.

† All authors contributed equally to this work.

* Corresponding author at: Schubertstrasse 42, D-01309 Dresden, Germany.
E-mail address: christian.beste@uniklinikum-dresden.de (C. Beste).

2213-1582/$ - see front matter
http://dx.doi.org/10.1016/j.nicl.2014.04.003

how this interaction then usually leads to impaired cognitive performance in Huntington's disease (Lawrence et al., 1998, 2000; Stout et al., 2001) is unknown.

A critical test for these hypotheses would require an examination of sensory decision-making processes in a neurological condition that is characterized by medium spiny neuron dysfunction but without the corresponding enhancement of NMDA receptor function. In this regard, benign hereditary chorea (BHC, MIM 118700) may serve as a model (for review see Kleiner-Fisman and Lang, 2007 and Inzelberg et al., 2011). BHC is a rare autosomal dominant disease (prevalence between 1 and 2 in 1,000,000 people), which is caused by mutations in the TITF1 gene on chromosome 14q13 encoding the thyroid transcription factor-1 (also known as TITF1, TEBP or NKX2-1) (Inzelberg et al., 2011). TTF1 mediates striatal interneuron migration from the medial ganglionic eminence (a precursor of the globus pallidus) to the lateral ganglionic eminence (a precursor of the striatum) (Sussel et al., 1999). This migration is reduced in TITF1 mutation and leads to dysgenesis of the formation of medium spiny neurons (Kleiner-Fisman et al., 2005; Yoshida et al., 2012). By contrast, TITF1 has no known role in NMDA receptor function (Sussel et al., 1999) and thus NMDA receptor function in BHC is likely unaltered.

Consequently, we tested a BHC patient and manifest Huntington's disease patients against age-matched controls to dissociate the contributions of striatal changes in NMDA sensitivity and network structure to enhanced response selection. Using a computational model of the striatum, we tested the hypothesis that either of these changes in the striatum could directly affect response selection, and then tested the hypothesis that increased NMDA sensitivity in the striatum of Huntington's disease patients could enhance selection despite the loss of neurons. Critically, we sought from the model the key explanation for the paradox of why both impaired (Jahanshahi et al., 1993; Lawrence et al., 1998) and enhanced response selection could arise in Huntington's disease.

2. Materials and methods

2.1. Patients and participants

A group of manifest Huntington's disease patients ($N = 10$; 6 females) between 20 and 40 years of age (mean age 33.45 ± 5.5) without any medication and a group of controls ($N = 10$; 6 females) matched to the manifest Huntington's disease group in age, sex and educational background were recruited. Along with these groups, a case of benign hereditary chorea (BHC) (female, 24 years of age) with strong motor symptoms was recruited and compared to the other groups using single-case *t*-statistics (Crawford and Garthwaite, 2012). BHC was genetically confirmed by detecting the mutation in the TTF1 gene and the BHC case did not take any medication at the time point of examination. The clinical and neuropsychological test data of these groups and the BHC case are shown in Table 1. The study was approved by the Ethics Committee of the Ruhr-University of Bochum. The study was conducted according to the Declaration of Helsinki. All participants and the BHC case gave written informed consent.

2.2. Task

Subjects performed a distraction paradigm (Beste et al., 2008; see also Schröger and Wolff, 1998) in which tones at three different frequencies (1000 Hz, 1100 Hz, 900 Hz) were presented for either 400 or 200 ms. One pitch (i.e., 1000 Hz) served as the standard tone, which was presented in 80% of trials. The other pitches were presented with a frequency of 10% each. The subjects were asked to respond with their thumb and indicated, whether the tone was short (right button press) or long (left button press). Variations in the pitch of the tone thus served as distraction.

2.3. EEG recording and analysis

The EEG was recorded from 32 scalp electrodes at standard positions according to the 10/20 system. Electrode signals were sampled at 1000 Hz with Cz as primary reference. The resulting time-series were downsampled to 256 Hz in offline post-processing and re-referenced to linked mastoids. After a first visual inspection of the time-series a bandpass filter from 0.5 to 20 Hz (48 dB/oct) was applied. Ocular artefacts (blinks and saccades) as well as pulse artefacts were corrected using independent component analysis (Infomax algorithm), applied to the un-epoched time-series. Besides the MMN, other processes related to the reorientation of attention (RON (Schröger et al., 2000)) have also been found to be increased in their efficacy in Huntington's disease, whilst attentional shifts (reflected by the P3a; Escera and Corral, 2007) are not affected (Beste et al., 2008). If exaggerated glutamatergic neural transmission is of similar importance for reorientation processes, the RON and P3a mechanisms should be similarly modulated to the MMN. To measure the MMN, P3a and the RON the EEG time-series were epoched in segments from −200 till 800 ms after the stimulus onset. Within these epochs an automated artefact rejection procedure was applied. Rejection criteria included a maximum voltage step of more than 60 μV/ms, a maximal value difference of 150 μV in a 250 ms interval or activity below 0.1 μV. After this, a baseline correction was −200 till 0 (i.e., time point of stimulus presentation was applied). To measure the MMN, P3a and RON, difference waves were calculated (distractor minus standard ERPs) (Kujala et al., 2007). In these difference waves the MMN was defined as the most negative peak between 100 and 250 ms. The P3a was defined as the most positive peak between 250 and 500 ms and the RON was defined as the most negative peak between 400 and 600 ms post-stimulus presentation. The ERPs and the behavioral data are shown in Fig. 1.

2.4. Statistical tests

Behavioural data of the BHC case in relation to the Huntington's disease group and controls were analysed using single-case *t*-statistics (Crawford and Garthwaite, 2012) applying Crawford and Howell's method. This method is widely used and offers the best possible way to compare single cases with groups of other subjects (for review see Crawford and Garthwaite, 2012). ANOVAs were used to examine effects between the Huntington's disease and control groups. Post-hoc tests in the Huntington's disease and control group were Bonferroni-corrected where necessary. All descriptive statistics are given as mean and standard error of the mean.

2.5. Population model of competing striatal populations

We used reduced models of the striatal microcircuit (Figs. 2 and 3) to understand the mechanisms by which Huntington's disease- and BHC-like changes in the striatum could potentially alter selection. In the baseline model, each medium spiny neuron population's firing rate a was modelled as a leaky integrator of inputs from the cortex and other medium spiny neuron population:

$$\tau \dot{a}_i = -a_i + w_{ji}\lfloor a_j \rfloor^+ + w_I I_i \quad (1)$$

$$\tau \dot{a}_j = -a_j + w_{ij}\lfloor a_i \rfloor^+ + w_I I_j \quad (2)$$

which decays with time constant τ, and is driven by the sum of weighted cortical input I_i,I_j and feedback inhibition (w_{ij},$w_{ji} \leq 0$) from the other medium spiny neuron population. The operation $\lfloor \cdot \rfloor^+$ indicates that negative medium spiny neuron population activity is rectified to zero.

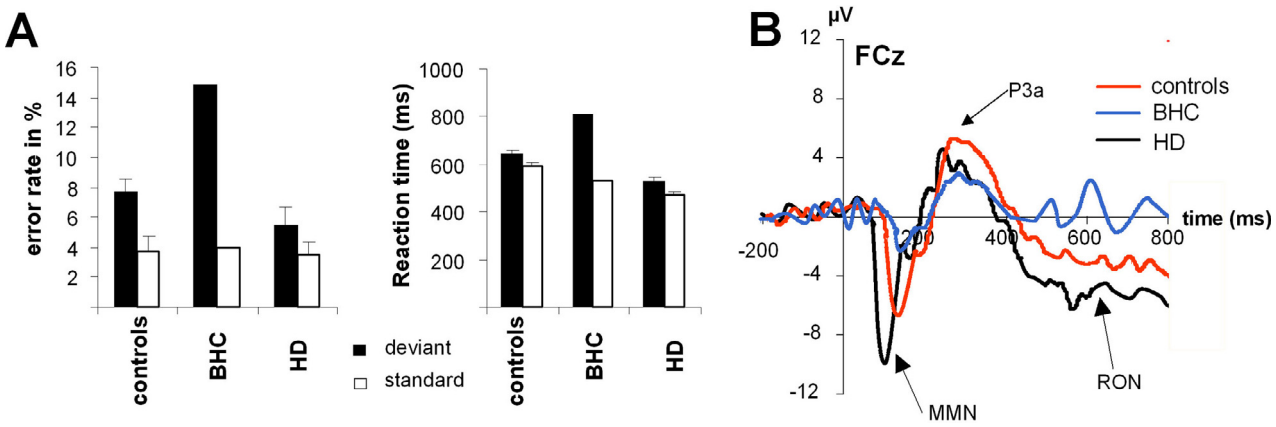

Fig. 1. Behavioural and electrophysiological differences in the auditory discrimination task. (A) Error rates and reaction times on distractor (black) and standard trials (white) in controls, manifest Huntington's disease and the BHC case (±SEM). The data shows better selection performance (fewer errors, faster reaction times) in Huntington's disease, but reduced selection performance in BHC, compared to controls. (B) Differences (standard minus distractor) at electrode Fz for controls (red), manifest Huntington's diseases (black) and BHC (blue). The different parts of the difference waves are labelled MMN, P3a and RON. Paralleling the behavioural data, the MMN and RON were increased in Huntington's disease and decreased in BHC, relative to controls.

Table 1
Description and analysis of performance (test scores) in different neuropsychological tests.

Test		BHC	HD	Controls	HD vs. controls	BHC vs. controls	BHC vs. HD
UHDRS motor score		26	24.5 (9.9)	NA			
CAG repeat length		NA	45.3 (5.5)	NA			
IQ (MWT-B)		105	103 (4.5)	113 (8.7)			
Stroop test (UHDRS)	Colour naming	61	48.5 (16.7)	81.1 (3.6)	***	***	**
	Colour reading	98	65.6 (14.9)	93.7 (5.1)	***		**
	Interference	36	30.5 (12.5)	52.1 (3.5)	***	***	**
Symbol–digit test (WAIS)		51	39.4 (10)	55.3 (3.4)	***		**
Word fluency (Benton)		39	26 (8.8)	46.2 (9.6)	***		**
Digit span (WMS-R)	Forward	8	5.1 (1.1)	9.1 (1.1)	***		**
	Backward	5	2.2 (0.9)	8.0 (0.9)	***		**
Block span (WMS-R)	Forward	8	4 (0.7)	8.7 (0.9)	***		**
	Backward	7	3.1 (0.5)	7.9 (0.9)	***		**
Benton test (visual memory)		11	7.6 (1.8)	13.5 (0.9)	***		**
Mini Mental Status Examination (MMSE)		30	28.5 (2.1)	30	***		**

Significances denote: $^{**}p < .01$. $^{***}p < .001$.

Extending this model to include the self-inhibition of each medium spiny neuron population gave:

$$\tau \dot{a}_i = -a_i + w_{ji}\lfloor a_j \rfloor^+ + w_I I_i + w_{ii}\lfloor a_i \rfloor^+ \quad (3)$$

$$\tau \dot{a}_j = -a_j + w_{ij}\lfloor a_i \rfloor^+ + w_I I_j + w_{jj}\lfloor a_j \rfloor^+ \quad (4)$$

where w_{ii},w_{jj} are the self-inhibition weights. This model is schematically illustrated in Fig. 3B.

Further extending this model to incorporate the feedforward inhibition of the medium spiny neuron populations by a population of fast spiking interneurons gave:

$$\tau \dot{a}_i = -a_i + w_{ji}\lfloor a_j \rfloor^+ + w_I I_i + w_{ii}\lfloor a_i \rfloor^+ + w_F I_F \quad (5)$$

$$\tau \dot{a}_j = -a_j + w_{ij}\lfloor a_i \rfloor^+ + w_I I_j + w_{jj}\lfloor a_j \rfloor^+ + w_F I_F \quad (6)$$

where $I_F = f(I_i,I_j)$ is the input received from the fast spiking interneuron population, and is some (strictly-increasing) function of the cortical inputs to the striatum. Given the dense connectivity of each fast spiking interneuron with their target medium spiny neurons (Humphries et al., 2010; Planert et al., 2010), we have assumed here a "broadcast" model in which the fast spiking interneuron population projects equally to the two competing medium spiny neuron populations with weight w_F. This model is schematically illustrated in Fig. 3C. We note that fast spiking interneurons do not express NMDA receptors and so are likely spared in Huntington's disease.

Inputs from the cortex emulated a pre-selection and a selection phase of a two-choice task; the success of selection was assessed in the selection phase. In the pre-selection phase both response-representing medium spiny neuron populations received from the cortex the same input r_{pre}, simulating the onset of task-salient information. In the selection phase, the first medium spiny neuron population received a step in input of r_{step}, simulating an increase in salience of that response after the perceptual decision was made (e.g.

the pushing of the left or right button after the decision on whether the tone was short or long).

The consequent output of the two medium spiny neuron populations was read-out in a signal selection framework (Gurney et al., 2001): we considered that the response was correctly selected if the output of the "winning" response population crossed a threshold θ_H above its steady-state and that the output of the "losing" response population crossed a threshold θ_L below it steady-state; otherwise we consider the selection to be ambiguous (the formal expression is given by Equations 6–7 of the Supplementary results). Here we assume that ambiguous response selection leads to both a potential error and an increased reaction time as the ambiguity must be instead resolved in the final common motor pathway to produce a motor output (Prescott et al., 1999). For all illustrative plots (Figs. 2–5) we use upper and lower thresholds of ± 2 Hz.

The D1–D2 model (Fig. 5) splits the two medium spiny neuron populations into two sub-populations of D1 and D2-expressing medium spiny neurons. The dynamical equations of each population were identical to those for the two-population models, except for the addition of input from all three other medium spiny neuron sub-populations (schematically illustrated in Fig. 5). This four-dimensional system did not allow for exact solution, and so results were obtained by numerical integration using the Euler numerical method. The time constant was arbitrarily set to $\tau = 1$, as it has no effect on the equilibrium state. To enable direct comparison, all weights were set to the same values as those used to generate the illustrative analytical results in Fig. 3: lateral and self-inhibition weight $= -0.5$; fast spiking interneuron input weight $= -0.1$.

2.6. Biophysical model of competing striatal populations

We examined whether or not the introduction of non-linear neuronal dynamics would alter the conclusions from the reduced model by constructing a canonical microcircuit model. Our biophysical model replicated the reduced fast spiking interneuron feed-forward inhibition model as this was the most complete model we examined. The biophysical model also provided a strong test of the striatum's ability to perform signal selection as it explicitly incorporated the weak synaptic efficacy of medium spiny neuron local collateral connections and the realistic connection densities of the striatal circuit.

Two model medium spiny neurons represented the output of two small medium spiny neuron populations encoding two alternative responses. They received spike train input from two cortical populations encoding the salience of the alternative responses. The other components of the model simulated spiking input from the other medium spiny neurons and from the fast spiking interneurons of the striatum (Tepper et al., 2004).

We used the spiking medium spiny neuron model from Humphries et al. (2009a), which reproduces characteristic behaviour of these neurons including their f–I curves, slow-rise to first spike on current injection, and paired-pulse facilitation. AMPA and GABAa induced post-synaptic currents were modelled as standard single exponential functions of short decay. As NMDA receptors are primarily affected in Huntington's disease, we used a detailed NMDA synaptic current model including voltage-dependent block by magnesium ions and saturation (full equations and parameters of the biophysical model neuron are given in the Supplementary methods). Enhanced NMDA receptor sensitivity was modelled by increasing the NMDA receptor conductance.

Each of the cortical, fast spiking interneuron, and medium spiny neuron populations were simulated as a generator of spiking input to the model medium spiny neurons, producing the spike-events that occur across N afferents to the medium spiny neuron. Given time-step Δt (s) and mean spike rate r (spikes/s), the probability of a spike per afferent is $p(s) = r\Delta t$. The total number of spike-events S at each time-step is then just drawn from a binomial distribution $S = B(N,p(s))$. The resulting time-series of spike-events is equivalent to the pooling of N spike trains modelled as independent renewal processes.

For the cortex, two generators were used with mean rates r_1 and r_2. Following arguments in Humphries et al. (2009b) for the size of the active afferent cortical population to one medium spiny neuron we set $N = 500$ for both. For the feed-forward fast spiking interneuron population, the mean rate was based on the rate of cortical firing. We simulated our large-scale network model of the striatum (Humphries et al., 2010) with a range of cortical inputs to determine the fast spiking interneuron population's input–output function. When simulating the biophysical microcircuit model, we took the mean of the cortical inputs and r_2 and looked up the corresponding mean fast spiking interneuron rate from the derived input–output function. We assumed a density of 1% fast spiking interneurons in the striatum, which gives $N = 31$ fast spiking interneurons afferent to 1 medium spiny neuron (Humphries et al., 2010).

The feedback medium spiny neuron population's mean rate was based on the output of the two neuron models. We took the mean of their spike-rate over a 1 s window. The medium spiny neuron feedback was turned on after 1.5 s to allow stable firing to develop. We used $N = 728$ medium spiny neurons afferent to 1 medium spiny neuron (Humphries et al., 2010). Excitotoxic death of medium spiny neurons in Huntington's disease and loss of medium spiny neuron local fibres in BHC were modelled as a reduction in the size of this feedback population.

The task-emulating inputs to the biophysical model had the same protocol as those for the reduced model (see above), with the only difference being that the cortical input was now explicitly given as spiking input. Here we used $r_{pre} = 2$ Hz (giving 1000 spikes/s total input to each medium spiny neuron). The step was made at 7 s, and firing rate estimates were made in 5 s windows before and after the step. The long durations in the biophysical model were used only to allow accurate assessment of firing rates from the resultant spike trains of the two model neurons.

As reported in the Results section, we searched for the minimum step-size that would achieve unambiguous signal selection. For each increment of the search, we increased the input step by 0.05 spikes/s per cortical train, and repeated the full simulation 20 times. Across these simulations we computed the mean firing rate in the post-step window for both the winning and the losing medium spiny neuron population, and compared to the upper and lower thresholds. The search was halted once both thresholds were crossed. When comparing minimum step-sizes between models (Fig. 4B), we considered them different if there was a greater than ± 1 SEM overlap between the mean values.

3. Results

3.1. Striatal disorders have opposite effects on task performance

We used a simple auditory decision task to probe the effects of striatal disorders on response selection. On every trial subjects were asked to indicate which of a short (200 ms) or long (400 ms) tone was played; 20% of trials had an irrelevant change in pitch as a distractor. The task was carried out by a group with manifest, non-medicated Huntington's disease ($n = 10$), a matched control group ($n = 10$), and a single BHC patient. Compared to the control group and BHC patient, the Huntington's disease group was impaired on a range of standard cognitive tasks (Table 1).

The Huntington's disease and control groups were newly tested, and so also acted as a stringent test that we could replicate our previous surprising results showing enhanced response selection in Huntington's disease patients (Beste et al., 2008). We found that the three groups differed in their error rates, but only on distractor trials (Fig. 1). Error rates were generally higher for distractor trials (7.4 ± 0.47%) compared to standard trials (3.93 ± 0.11%) ($F(1,18) = 41.00$; $p < 0.001$; =0.695).

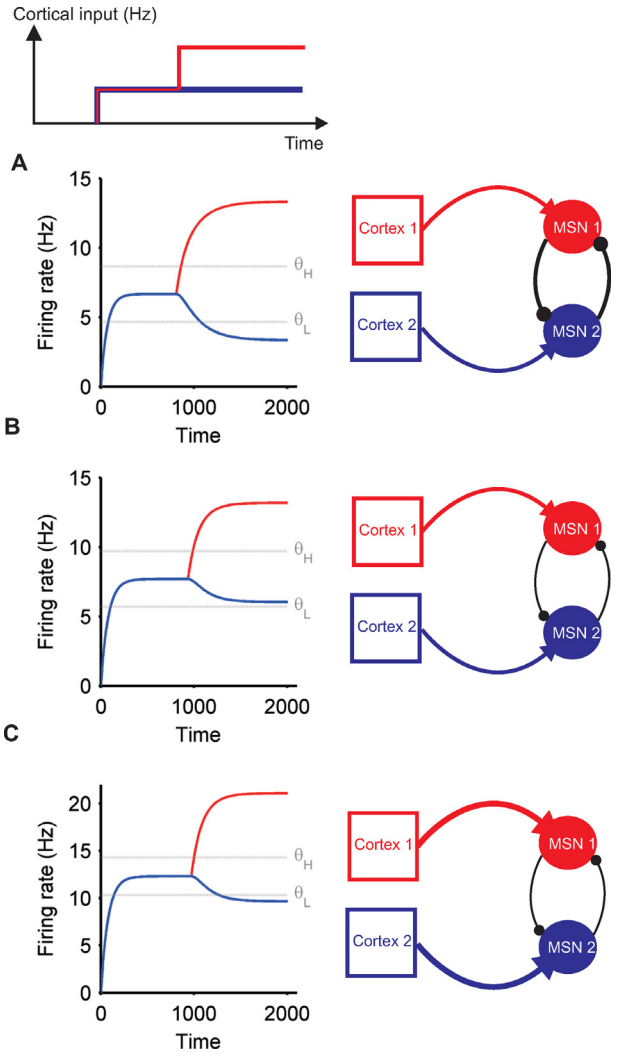

Fig. 2. Signal selection in healthy-state, Huntington's disease-like and BHC-like models of the striatum. The medium spiny neuron (MSN) populations receive inputs representing competing response signals, with the more salient response having a step increase (top); response selection is read-out from the population outputs after the step, by checking that both upper (θ_H) and lower (θ_L) thresholds are crossed. All example simulations show responses to the same input. (A) The healthy-state model. Line-widths in the model schematic (right) indicate relative synaptic weights. (B) A BHC-like model, with loss of medium spiny neuron intra-connectivity. (C) A Huntington's disease-like model, with loss of medium spiny neuron intra-connectivity due to cell death and enhanced cortical input weight due to increased NMDA receptor sensitivity.

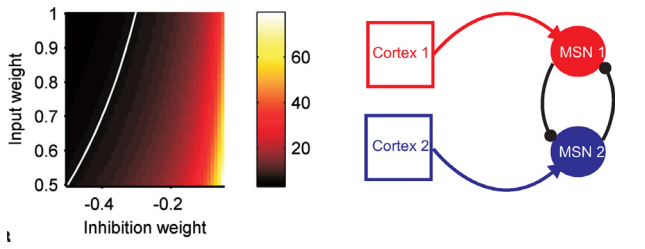

Fig. 3. Selection by the striatum is differentially modulated by increased NMDA sensitivity and loss of striatal connectivity. In each panel, we show a schematic of the model circuit (right), and the analytically-computed minimum input step required for unambiguous signal selection (left) as a function of the inhibitory and input weights. Each heat map's colour intensity encodes the required minimum input step (firing rate, in Hz) for those weights, and the white line is the analytical boundary that separates the regions of smaller (above) and larger (below) step-sizes than the healthy-state model (bottom left-hand corner). Heat maps are plotted for specific choices of model parameter values to illustrate the general insights from the analytical solutions (Supplementary results), and so these results do not depend on specific choices of parameter values. (A) The baseline model of weakly-competing medium spiny neuron (MSN) populations. (B) The effect of adding inhibitory feedback to competing medium spiny neuron populations. (C) The effect of adding feed-forward inhibition from fast spiking interneurons (FSIs) to competing medium spiny neuron populations. The fast spiking interneuron population is a "broadcast" model that equally samples from the cortical inputs and equally outputs to the medium spiny neuron populations.

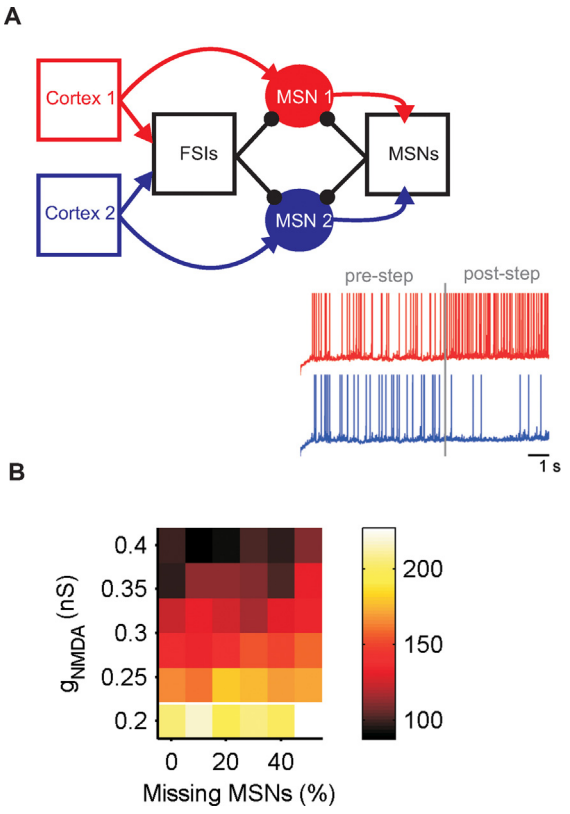

Fig. 4. Tradeoff between increased NMDA sensitivity and decreased striatal connectivity is robust to nonlinear neuronal dynamics. (A) The reduced spiking microcircuit model. Two spiking model medium spiny neurons (red, blue) represent the two populations of medium spiny neurons (MSNs). Each neuron model receives glutamatergic input (arrows) via AMPA and NMDA receptors from its afferent cortical populations, and GABAergic input (circles) from striatal fast spiking interneurons (FSIs) and from the other medium spiny neurons. Each box represents a source of spikes based on the number of spikes received from the indicated sources. The numbers of connections between each indicated population are derived from a full three-dimensional model of striatal micro-anatomy (Humphries et al., 2010)). Inset: an example of the output of the two medium spiny neuron models during a single selection test. Cortical input to MSN1 increased at 7 s (grey line), representing a more salient response signal. (B) Landscape of minimum input step required for unambiguous signal selection (in total spikes/s from cortical spike-trains). The value for each parameter pair (missing medium spiny neurons, NMDA conductance) is the mean of 20 numerical searches for the minimum input step. The white line gives the boundary between better (smaller step) and worse (larger step) signal selection performance than the healthy-state model (bottom left).

The mixed effect ANOVA (standard vs. distractor as within-subject factor, Huntington's disease vs. control as between subject factor) revealed an interaction "standard/distractor × group" ($F(1,18) = 14.19$; $p = 0.001$; =0.441). Post-hoc tests showed that the control and Huntington's disease groups did not differ on standard trials ($p > 0.6$) but did on distractor trials ($p < 0.001$), with Huntington's disease patients showing better performance compared to controls (cf. Fig. 1A). Importantly, the BHC patient was also less accurate on distractor trials, when compared to the control group ($t = 2.4$; $p = 0.019$) and Huntington's disease group ($t = 2.6$; $p < 0.01$). No difference between the BHC patient and the control or Huntington's disease groups was evident in standard trials ($p > 0.4$).

We found that the three groups also differed in their reaction times. A mixed effects ANOVA (standard vs. distractor as within-subject factor, Huntington's disease vs. control as between subject factor) showed that reaction times were faster on standard trials (574 ms ± 10.1) compared to distractor trials (613 ± 11.1 ms)

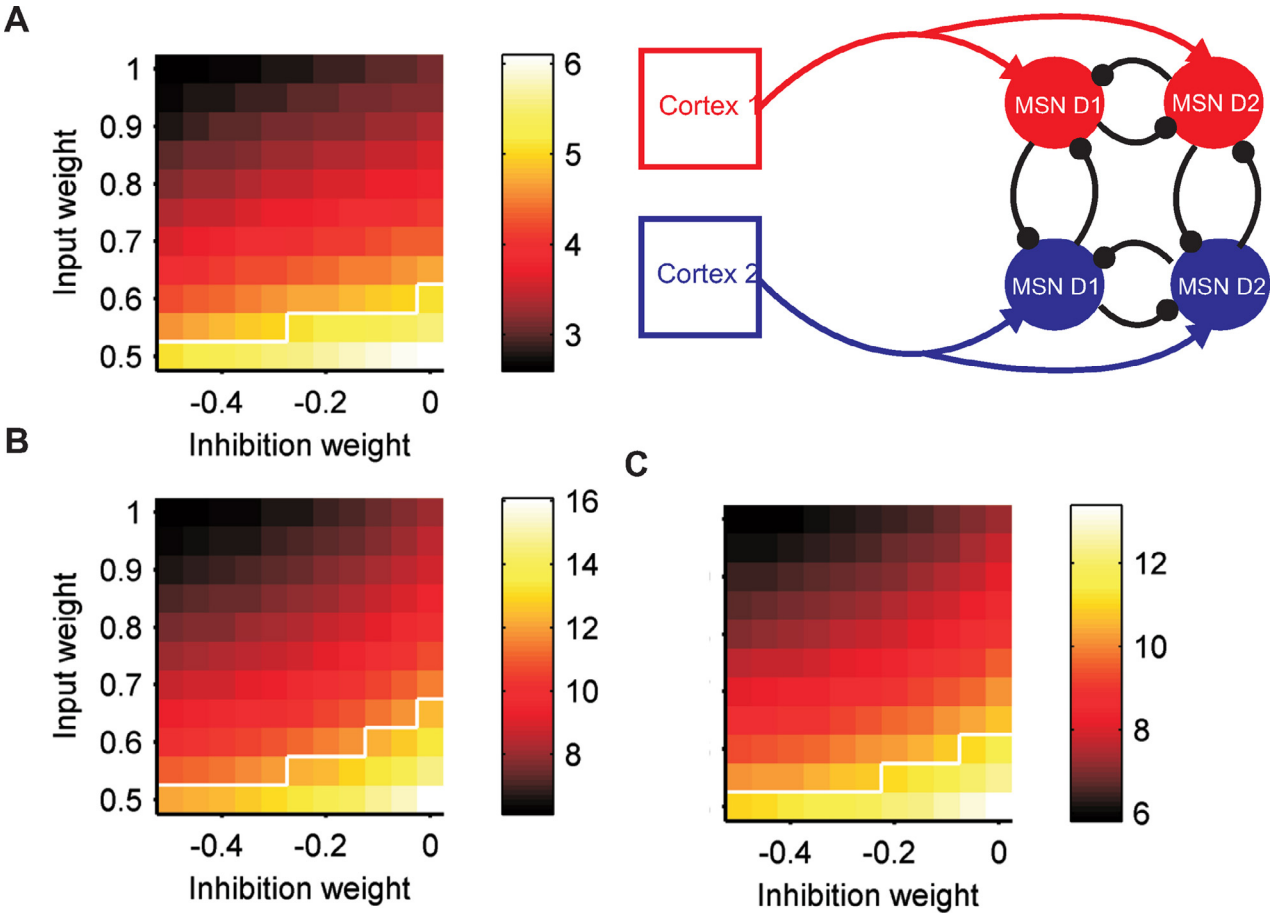

Fig. 5. Tradeoff between increased NMDA sensitivity and decreased striatal connectivity occurs for selective loss of D2 medium spiny neurons (MSNs). (A) The D1–D2 microcircuit model. Right: we split the two medium spiny neuron populations into separate sub-populations of medium spiny neurons predominantly expressing the D1 and D2 receptors for dopamine, and modelled the resulting connections within and between them. Both the D1 and D2 medium spiny neuron populations received the same input signal from their corresponding cortical population; the selection was read-out from the D1 medium spiny neuron population's output. Left: minimum input needed to achieve unambiguous signal selection following selective loss of the D2 medium spiny neurons only: all D2 medium spiny neuron output weights were changed whilst the D1 medium spiny neuron output weights were held constant. Heat map conventions are the same as in Fig. 3; the results plotted here are from numerical simulations. (B) The D1–D2 microcircuit model with the addition of feedback self-inhibition to each medium spiny neuron population: the heat map gives the minimum input needed to achieve unambiguous signal selection following selective loss of the D2 medium spiny neurons only. (C) The D1–D2 microcircuit model with the further addition of feed-forward fast spiking interneuron (FSI) input to each medium spiny neuron population: the heat map gives the minimum input needed to achieve unambiguous signal selection following selective loss of the D2 medium spiny neurons only.

($F(1,18) = 7.62$; $p = 0.013$; $=0.297$). There was no interaction "standard/distractor × group" ($F(1,18) = 0.03$; $p > 0.9$), but the main effect group revealed that the Huntington's disease group showed faster responses (550 ± 11.8 ms) than the control group (637 ± 12.1 ms) ($F(1,18) = 27.02$; $p < 0.001$; $=0.600$). For the BHC patient, the single-subject *t*-tests (see Materials and methods) revealed that in distractor trials reaction times were longer compared to those in both the control group ($t = 3.11$; $p < 0.006$) and the Huntington's disease group ($t = 5.26$; $p < 0.001$), but not in standard trials ($p > 0.5$).

3.2. Performance changes have specific neural correlates in EEG

The electrophysiological data (difference wave ERPs) (MMN, P3a and RON) for the control group, Huntington's disease group and BHC patient are shown in Fig. 1B. The mismatch negativity (MMN) was analysed at electrode Fz (e.g. Näätänen et al., 2012). Here, the Huntington's disease group revealed a larger MMN (−9.99 ± 0.66 μV) compared to the control group (−7.32 ± 0.45 μV) (univariate ANOVA; $F(1,18) = 17.68$; $p = 0.001$; $=0.496$). The latency of the MMN was shorter in the Huntington's disease group (119 ± 6.5 ms) compared to the control group (152 ± 5.5 ms) ($F(1,18) = 14.63$; $p = 0.001$; $=0.448$). Importantly, the BHC patient revealed a smaller MMN (−3.12 μV) compared to the Huntington's disease group ($t = 4.51$; $p < 0.001$) and the control group ($t = 2.81$; $p = 0.01$). In the BHC patient, the MMN latency (160 ms) was longer compared to that in the Huntington's disease group (119 ± 6.5 ms) ($t = 2.17$; $p = 0.02$), but not different to controls ($p > 0.4$). For the P3a measured at electrode Fz, there was no difference between the Huntington's disease group, control group and BHC patient (all $p > 0.5$). For the RON, however, the pattern of results was identical to that in the MMN data. For the RON, the amplitude was larger (most negative) for the Huntington's disease group (−7.85 ± 0.6 μV) compared to the control group (−4.82 ± 0.61 μV) ($F(1,18) = 12.83$; $p = 0.002$; $=0.416$). The RON in the BHC patient (0.2 μV) was less negative compared to that in both the control group ($t = 2.86$; $p = 0.009$) and Huntington's disease group ($t = 3.67$; $p = 0.002$).

3.3. Hypotheses for response selection in the striatal microcircuit

The disorders caused opposite changes in response selection compared to controls: reduced errors and response time for Huntington's disease patients (replicating our previous study, Beste et al., 2008);

increased errors and response time for the BHC patient. The electrophysiological data showed significant differences in event related potentials between the Huntington's disease group, control group, and BHC patient, confirming that the performance differences reflected changes in neural processing.

We propose that this dissociation between Huntington's disease and BHC effects on response selection supports two hypotheses. First, that as both disorders predominantly affect the striatum, so computational processes involving the striatum directly influence the observed response selection; it thus follows that changes in the striatum are the cause of changes in this selection. Second, that as both disorders cause changes to the striatal network, the selection enhancement seen in Huntington's disease patients is solely due to enhanced NMDA sensitivity in the striatum.

We simulated a striatal microcircuit model to test these hypotheses. To address the first hypothesis we sought to show how selection could be either impaired or enhanced at the level of the striatal microcircuit itself. We further sought from the model a potential explanation for the key challenge: why, if our hypotheses are correct, Huntington's disease patients are usually impaired compared to controls in other decision-making tasks. Consequently, we focussed here on modelling the generic striatal mechanisms for response selection potentially common to a range of tasks.

3.4. Computational analysis of enhanced and impaired response selection

We first show analytically how Huntington's disease-like and BHC-like changes affect response selection in a reduced model of weakly-competing medium spiny neuron populations. We then show the robustness of these results to variations in the striatal circuitry, to the addition of biophysical details that may affect selection processes, and to the selective loss of striato-pallidal cells in Huntington's disease.

3.5. Enhanced NMDA sensitivity compensates for depletion of striatal connectivity

The computational role of the striatum is contentious. The presence of local collateral connections between the GABAergic medium spiny neurons seems consistent with a winner-take-all computation on its inputs (Beiser et al., 1997), but the winner-take-all hypothesis has been undermined by the weakness of the synapses formed by these local collaterals (Jaeger et al., 1994; Czubayko and Plenz, 2002; Tunstall et al., 2002; Taverna et al., 2004). However, winner-takes-all is an extreme of a continuum of selection computations (Fukai and Tanaka, 1997). A more general form is signal selection, where an unambiguous selection between competing signals is indicated by the winning signal rising above an upper threshold and the losing signal(s) falling below a lower threshold. The existence of many weak medium spiny neuron inputs to each medium spiny neuron is potentially sufficient to collectively influence its output (Humphries et al., 2010; Chuhma et al., 2011; Yim et al., 2011). We also note that, as the primate striatum is predominantly silent (Hikosaka et al., 1989), to see competition between medium spiny neuron populations would need a task invoking strong cortical inputs to those populations. Under these conditions, even weakly competitive medium spiny neurons are capable of modulating signal selection (Supplementary results, Section 1.1). We show here that this signal selection is modulated by Huntington's disease-like and BHC-like changes.

We constructed a reduced model of two weakly competitive medium spiny neuron populations representing alternative responses (Materials and methods). Input to the model represents the putative cortical signals for the salience of the two potential responses (short/long) on one trial: at the onset of the auditory tone, both inputs are set to some non-zero value, indicating that only these responses are salient. A further step in input to one medium spiny neuron population then represents the decision-point at which the short/long percept is resolved (Fig. 2, top), and indicates the increased salience of the corresponding response.

The output of the two medium spiny neuron populations after the step in input was read-out for signal selection (Fig. 2). Fig. 2A shows an example of signal selection by the medium spiny neuron population output for the healthy-state model. We compared the performance of this model to BHC-like and Huntington's disease-like models that emulated the changes to the striatal microcircuit thought to occur in these disorders. The loss of inter-medium spiny neuron connectivity in Huntington's disease (due to medium spiny neuron cell death) and BHC (due to depletion of medium spiny neuron local collaterals) was emulated by reducing the lateral inhibition weights between the two populations (Fig. 2B). The increased NMDA sensitivity in Huntington's disease was emulated by increasing the weight of input from the cortex to the two medium spiny neuron populations (Fig. 2C). Fig. 2B and C illustrates how example BHC- and Huntington's disease-like changes altered the signal selection performance compared to the healthy-state model.

To understand the impact of these Huntington's disease- and BHC-like changes, we quantified response selection performance by finding the minimum step change (ΔI) in cortical input needed to get unambiguous signal selection. This value thus indicates the difficulty of the selection process, and we could then quantify how that difficulty changes with alterations to the microcircuit. We exactly solved the models to find the minimum input step required in the healthy-state model, and after all possible BHC-like and Huntington's disease-like changes to the microcircuit (Supplementary results, Section 1).

We find that, given the two thresholds (θ_H, θ_L) for unambiguous signal selection, the minimum step in input to reach both is

$$\Delta I = \frac{\theta_L \left(1 - w_{ij} w_{ji}\right)}{w_I w_{ij}} \tag{7}$$

where w_I is the cortical input weight, and (w_{ij},w_{ji}) are the lateral inhibition weights between the two medium spiny neuron populations (note that only the lower threshold θ_L appears in this function, as the step-size needed to reach that threshold is always at least as big as that needed to reach the upper threshold — see Supplementary results, Section 1.2).

Eq. (7) shows that loss of connectivity between medium spiny neuron populations, reducing the magnitude of w_{ij} and w_{ji}, always increased the minimum step size, indicating impaired selection compared to the healthy-state model. This is consistent with the BHC patient's poor selection performance compared to controls. Conversely, Eq. (7) shows that solely increasing the cortical input weight (w_I) decreased the minimum step size, indicating comparatively enhanced selection compared to the healthy-state model. The heat map in Fig. 3A illustrates these main analytical insights by plotting the dependence of the minimum input step (in Hz) needed for unambiguous signal selection on the reduction in lateral inhibition weight and the increase in cortical input weight; the healthy-state model is given at the lower-left corner.

In the Huntington's disease-like case, both decreased medium spiny neuron connectivity and increased cortical input weight occur simultaneously. Given some change in medium spiny neuron population connectivity from (w_{ij},w_{ji}) in the healthy-state to (w^*_{ij}, w^*_{ji}) in the Huntington's disease-like state, we can determine from the model (Supplementary results, Section 1.2) the value of the cortical input weight w^*_I needed to exactly compensate and maintain the same selection performance:

$$w^*_I = \frac{w_I w_{ij} \left(1 - w^*_{ij} w^*_{ji}\right)}{w^*_{ij} \left(1 - w_{ij} w_{ji}\right)}. \tag{8}$$

We plot an example of this function as the white line in the heat map of Fig. 3A. We can immediately see that Eq. (8) defines a critical threshold for increased NMDA sensitivity that separates states of "enhanced" and "impaired" selection compared to the healthy-state model. In the enhanced state, sufficiently increased NMDA sensitivity can still result in enhanced selection despite loss of medium spiny neuron inter-connectivity (region above the white line in the heat map of Fig. 3A).

This is consistent with the Huntington's disease patients' enhanced selection performance compared to controls. The analytical results (Eqs. (7) and (8)) show that the changes in selection due to changes in lateral inhibition and input weights, and therefore also this trade-off between them, exist irrespective of particular choices of threshold or weights. Therefore, our reduced model provides evidence for both our hypotheses: first, that the striatum can implement a selection process and thus directly influence response selection; second, that selection enhancement seen in Huntington's disease patients is solely due to enhanced NMDA sensitivity.

Moreover, our analytical results show that the impaired state also must always exist, in which insufficiently increased NMDA sensitivity will result in impaired selection through the loss of medium spiny neuron intra-connectivity (region below the white line in the heat map of Fig. 3A). The existence of this region is crucial: after all, in most simple decision-making tasks Huntington's disease patients' performance is significantly worse than control subjects (Lawrence et al., 1998), and so a model predicting a uniformly improved performance through increased NMDA sensitivity would be inconsistent with the proposed role of the striatum in response selection (implications of this are considered further in the Discussion section).

3.6. Trade-off of NMDA sensitivity and connectivity loss is robust to details of the striatal circuit

Our model of weakly-competing medium spiny neuron populations provided evidence for our two hypotheses, but other sources of inhibition of medium spiny neurons within the striatum raised two open questions: first, whether they prevented signal selection from occurring at all; second, even if signal selection was maintained, whether the Huntington's disease- and BHC-like models still showed signal selection changes that were consistent with the behavioural data.

We first examined the role of self-inhibition by each medium spiny neuron population. Local collateral connections in the above model are restricted to those between response-representing populations. Whilst this provides a baseline model for quantifying the effect of mutual competition on response selection, there is no a priori reason to suppose that medium spiny neurons in the two populations selectively connect only to medium spiny neurons in the other population: thus it is likely that medium spiny neurons within each population are also connected by local collaterals and consequently each population is self-inhibiting. We thus implemented a model incorporating feedback inhibition of each medium spiny neuron population (Fig. 3B).

We found that adding such self-inhibition does not alter the qualitative effects of losing connectivity between medium spiny neurons and of enhanced NMDA sensitivity (Supplementary results, Section 2.1). As an illustration of these results, Fig. 3B shows that self-inhibition increases the minimum input step needed compared to the baseline model, but the critical threshold separating model states with enhanced and impaired selection remains (Supplementary results, Eq. 16). Consequently, even with self-inhibition of the response-representing populations, BHC-like changes always lead to impaired selection, and Huntington's disease-like changes can lead to enhanced selection, again providing evidence for our two hypotheses.

Short time-scale dynamics in the striatum are strongly dependent on feed-forward input from GABAergic fast-spiking interneurons to the medium spiny neurons (Tepper et al., 2004; Mallet et al., 2005;Humphries et al., 2009b, 2010). Thus we also examined its potential influence on the striatal circuit's response selection ability, and how that ability is altered by Huntington's disease- and BHC-like changes. Given the extensive collateralization of the fast spiking interneuron axon and the vast number of medium spiny neurons each fast spiking interneuron contacts (Humphries et al., 2010; Planert et al., 2010), there is no a priori reason that a population of fast spiking interneurons would preferentially connect to one local medium spiny neuron population . Thus we implemented a "broadcast" model in which a population of fast spiking interneurons projects in equal proportion to both the medium spiny neuron populations representing alternative responses (Fig. 3C).

We found that introducing such feed-forward inhibitory input does not alter the qualitative effects of losing connectivity between medium spiny neurons and of increased NMDA sensitivity (Supplementary results, Section 2.2). As an illustration of these results, Fig. 3C shows that feed-forward inhibition from the fast spiking interneurons decreases the minimum input step needed compared to the baseline model (see Supplementary results, Section 2.2 for further discussion), but the critical threshold between model states showing enhanced and impaired selection remains (Supplementary results, Equation 24). Consequently, even with feed-forward inhibition of the response-representing populations, BHC-like changes always lead to impaired selection, and Huntington's disease-like changes can lead to enhanced selection, again providing evidence for our two hypotheses.

3.7. Trade-off of NMDA sensitivity and connectivity loss is robust to nonlinear neuronal dynamics

Such reduced models allow us a deep understanding of the microcircuit's dynamics, but cannot account for the potential contributions of non-linearities in single neuron dynamics. Three non-linear processes are particularly relevant for our understanding of the striatal microcircuit in Huntington's disease and BHC conditions: the non-linear voltage-dependent activation and the long-lasting saturation of the NMDA receptors, and the reversal potential of GABAa receptors.

As Huntington's disease is thought to lead to over-sensitive NMDA receptors (Fan and Raymond, 2007; Okamoto et al., 2009; Milnerwood et al., 2010), the first two processes are directly involved in how excitability of the medium spiny neuron changes in Huntington's disease. Their voltage-dependence means that the NMDA receptors become increasingly available for activation as the neuron's membrane potential is increased towards its firing threshold (Jahr and Stevens, 1990); this process feeds back on itself, whereby activation of some NMDA receptors depolarizes the neuron, which in turn makes further NMDA receptors available. In this way, NMDA receptors can non-linearly amplify the effects of small depolarizing inputs. The saturation of the NMDA receptors provides a ceiling on activity: as the neurotransmitter blocks the receptor for around 100 ms, so the receptor is unavailable for further activation by incoming spikes from pre-synaptic sources (Lester et al., 1990). In this way, NMDA receptors can non-linearly reduce the effects of changes at high pre-synaptic firing rates.

The reversal potential of GABAa synapses impacts the ability to perform selection, as the GABAergic connections between medium spiny neurons are not simply providing inhibition to each other (Plenz, 2003). The GABAa reversal potential is typically −60 mV and so is above the medium spiny neuron resting potential (typically −80 to −90 mV) (Plenz, 2003; Bracci and Panzeri, 2006). Consequently, GABAergic input from other medium spiny neurons and fast spiking interneurons produces excitatory potentials in medium spiny neurons at rest and only produces inhibitory effects once the medium spiny neuron is sufficiently depolarized.

To examine the potential contribution of these non-linear phenomena, we constructed a new biophysical model of the striatal microcircuit that incorporated a spiking medium-spiny neuron model with AMPA, NMDA, and GABAa receptors (Humphries et al., 2009a). The microcircuit model incorporated all three inhibitory connections examined in the reduced model: feedback inhibition between the medium spiny neuron populations, self-inhibition of the medium spiny neuron populations, and feed-forward inhibition from a fast spiking interneuron population (Fig. 4A).

To isolate the contribution of single neuron dynamics from connectivity effects, we used a single model neuron per medium spiny neuron population, and modelled all other connection as sources of spike train inputs. We simulated the increased NMDA sensitivity of medium spiny neurons in Huntington's disease by increasing the NMDA receptor conductance in the medium spiny neuron models, and simulated medium spiny neuron loss (in Huntington's disease) and connectivity loss (in BHC) by reducing the number of inputs received from the global medium spiny neuron population.

We found that this model reproduced the signal selection ability of the reduced model: a sufficiently large step in input to one population could cause that population's output to reach an upper threshold and the other population's output to reach a lower threshold. As the density of connections between the medium spiny neurons and from the fast spiking interneurons to the medium spiny neurons was derived from a detailed three-dimensional model of striatal anatomy (Humphries et al., 2010), and the synaptic conductances of these connections were taken directly from data (Koos et al., 2004; Gittis et al., 2010), this finding supports the above assertion that many, weak medium spiny neuron connections can produce signal selection.

We found that our biophysical model qualitatively reproduced the results of the reduced model (Fig. 4B): increased NMDA sensitivity reduced the minimum input step needed for unambiguous response selection, whereas decreased medium spiny neuron connectivity generally increased the minimum input step needed for unambiguous selection. Moreover, there existed two model states, one with enhanced selection through sufficiently increased NMDA sensitivity to compensate for loss of medium spiny neuron connectivity, and one with impaired selection. Thus, our hypotheses for striatal competition contributing to response selection and for increased NMDA sensitivity leading to enhanced response selection are not dependent on assumptions of linearity of the medium spiny neuron's dynamics.

3.8. *Selective vulnerability of indirect pathway striatal neuron populations still leads to trade-off*

A hallmark of the progression of Huntington's disease is that the D2-receptor expressing medium spiny neurons projecting to the external pallidum are lost more rapidly than the D1-receptor expressing medium spiny neurons projecting to the internal pallidum (Mitchell et al., 1999; Deng et al., 2004; Douaud et al., 2009). We thus also studied a reduced model incorporating this selective vulnerability. Each response-representing medium spiny neuron population was separated into its D1 and D2 receptor expressing sub-populations (Fig. 5A). Signal selection was read-out from the two D1 receptor sub-populations, as their target nuclei are thought to directly express selection of motor programs (Mink, 1996; Redgrave et al., 1999; Hikosaka et al., 2000).

Unlike the prior reduced model results (Fig. 3), analytical solutions are not available for this four-dimensional model and so numerical simulation was performed to find the minimum input step sufficient for unambiguous selection (Materials and methods).

To mimic the selective vulnerability of D2 medium spiny neurons in Huntington's disease, we looked at the effect on selection of reducing only the inhibitory weights originating from the D2 medium spiny neuron populations, whilst increasing the cortical input weight to both types of medium spiny neuron. This was intentionally an extreme characterization of the selective vulnerability, with no loss of D1 medium spiny neurons at all: we sought to check whether or not loss of neurons from a sub-population would have the reverse effect of non-selectively losing neurons from the whole population.

Fig. 5A shows that selectively losing only D2 medium spiny neurons increases the minimum input step required for selection, similar to the non-selective loss of medium spiny neurons. Moreover, Fig. 5A shows that correspondingly increased NMDA sensitivity in both D1 and D2 medium spiny neuron populations can still lead to the critical threshold between enhanced and impaired selection model states (white line in Fig. 5A). Neither the further addition of feedback self-inhibition for each sub-population (Fig. 5B) nor feed-forward inhibition from a fast spiking interneuron population to each sub-population (Fig. 5C) qualitatively changed these results. Thus, irrespective of the details of the microcircuit, if D2 medium spiny neurons are selectively vulnerable in Huntington's disease then their loss could still lead to impaired selection, which can be reversed by increased NMDA sensitivity.

4. Discussion

We tested patients with neurodegenerative disorders, including a rare case of BHC, against age-matched controls to dissociate the contributions of changes in the striatum to impaired and enhanced cognitive processes. Both the Huntington's disease patient group and the BHC patient had altered response selection on trials with irrelevant sensory information, providing further evidence that changes in the striatum affect selection (Beste et al., 2008). The disorders caused opposite changes in response selection compared to controls: reduced errors and response time for Huntington's disease patients (replicating our prior study, Beste et al., 2008); increased errors and response time for the BHC patient. Such deficits in cognitive functions in BHC are also shown in the neuropsychological test data (Stroop data) and are well in line with other results on cognitive functions in BHC (e.g. Gras et al., 2012).

In the electrophysiological data, these behavioural differences were reflected in a more negative MMN and RON for Huntington's disease patients (replicating our prior study, Beste et al., 2008), and a reduced MMN and RON for the BHC patient. The P3a did not show modulation across the examined conditions, which suggests that frontostriatal processes do not affect involuntary attentional shifting mechanisms in this paradigm.

Our results provide evidence that Huntington's disease and BHC have opposite effects on neural mechanisms for response selection: when medium spiny neuron dysfunction is combined with exaggerated glutamatergic neural transmission (as in manifest Huntington's disease), the efficacy of response selection increases. When medium spiny neuron dysfunction alone is evident (as in BHC), performance declines.

4.1. *Dissociated contributions of NMDA sensitivity and medium spiny neuron dysfunction to selection*

We proposed that this dissociation between Huntington's disease and BHC effects on response selection supports two hypotheses. First, that computational processes involving the striatum directly influence response selection in this task, and so changes in striatum are the cause of observed changes in selection. This is consistent with existing models and theories proposing that the striatum and the wider basal ganglia circuit underpin a general mechanism for selection (Mink, 1996; Redgrave et al., 1999; Plenz, 2003). Second, that the enhanced selection seen in Huntington's disease patients is solely due to enhanced NMDA sensitivity compensating for medium spiny neuron dysfunction.

Our computational model showed that increasing NMDA sensitivity indeed improved response selection compared to a healthy state model, whereas loss of medium spiny neuron local connections impaired response selection. Crucially, the model also showed how these changes to response selection account for the performance changes of both disorders: loss of medium spiny neuron local connections alone, as in BHC, only impaired selection; yet many combinations of increased NMDA sensitivity with consequent loss of medium spiny neuron local connections, as in Huntington's disease, improved response selection. Our model thus predicts a critical threshold at which increased NMDA sensitivity can more than compensate for the loss of medium spiny neurons in Huntington's disease, resulting in the observed enhanced cognitive processes.

We found that these results were robust to the details of the striatal microcircuit, to the selective vulnerability of the D2 medium spiny neuron population in Huntington's disease, and to the non-linear properties of NMDA and GABAa receptors. An open question is why the difference between groups was observed in the distractor trials only. A key insight from our analytical results was that the minimum input step needed for selection increased in the order: "enhanced" Huntington's disease-like state, the healthy state, and BHC-like state. Fig. S1 shows how this ordering of input steps provides a plausible hypothesis for the error rate changes both between groups and between trial types.

4.2. Enhanced or impaired selection is dependent on trade-off between sensitivity and cell loss

Importantly, our models all suggest that enhancement of selection only occurred in a sub-set of all possible Huntington's disease-like conditions. Our analytical results show that whether Huntington's disease-like models show enhanced or impaired response selection depends on whether or not NMDA sensitivity increases beyond a critical threshold for compensating the impairing effects of medium spiny neuron loss. Below this threshold, selection is worse than that for the healthy-state model. Our models thus predict that the normal impairment of Huntington's disease patients on a wide range decision-making tasks (Lawrence et al., 1998, 2000; Stout et al., 2001) is a consequence of NMDA receptor sensitivity not reaching this threshold.

As a corollary of this result, our model predicts that our simple auditory task engages a region of the striatum in the "enhanced" state, where medium spiny neuron cell loss is not too advanced compared to increased NMDA sensitivity. According to the excito-toxicity hypothesis (Fan and Raymond, 2007) the two processes are causally linked: the excessive exposure to glutamate underlying the increased NMDA sensitivity results in the death of medium spiny neurons. We would thus expect that there would be an upper limit on the increase in NMDA sensitivity before its consequent loss of medium spiny neurons dominates. Indeed, the existence of a dorsal–ventral gradient of striatal cell loss in Huntington's disease (Douaud et al., 2009) suggests that a gradient of trade-offs between sensitivity increases and cell loss is plausible. The region of the striatum supporting the enhanced performance is thus unlikely to be large: one possibility is that the auditory striatum plays a critical role in response selection in this task (Znamenskiy and Zador, 2013) and this region is in the "enhanced" state in Huntington's disease.

It is conceivable that effects are not restricted to the auditory striatum, because NMDA neural transmission and medium spiny neuron density have until now not been shown to differ between striatal subregions. In this regard recent molecular genetic association studies show that visual sensory memory is modulated by genetic polymorphisms encoding for neurotrophic factors and receptors highly expressed in the striatum and of relevance to glutamatergic neural transmission (e.g. Arning et al., 2014;Beste et al., 2012, 2011; Getzmann et al., 2013). However, we show that there could exist an "enhanced" selection state due to NMDA sensitivity compensating for cell-loss. But most studies show poor performance of Huntington's disease patients on response selection tasks. Our results suggest that in Huntington's disease most regions of the striatum are in the "impaired" state, leading to the poor performance, but that the auditory task engages a region of striatum that is in the enhanced state — and that region is not usually engaged in cognitive tasks, otherwise we would have seen this enhancement of performance before.

4.3. Potential limitations of the study

However, it has to be acknowledged that Huntington's disease is also accompanied by changes at the cortical level (e.g. Tabrizi et al., 2009), which was not taken into account in the model and which is clearly a limitation of the study. Obviously, these neocortical alterations may further modulate the results obtained. As stated in the Introduction section, TITF1 has no known role in NMDA receptor function (Sussel et al., 1999). Whilst this may be regarded as a weakness in the a priori assumption of the presented study and the computational model (i.e., that there is no evidence falsifying an affection of the NMDA receptor system in BHC), the experimental results presented for the Huntington's disease patients support the importance of the NMDA receptor system for sensory memory and perceptual decision making processes in line with other data (e.g. Javitt et al., 1996; Kreitschmann-Andermahr et al., 2001; Umbricht et al., 2002). The model simulations show that enhanced NMDA receptor involvement is critical for the effects to emerge. This, together with the fact that the BHC case and the Huntington's disease group reveal a completely dissociated pattern of results, replicating the pattern of a previous study (Beste et al., 2008), strongly suggests that NMDA receptor neurotransmission is likely to be unaltered in BHC.

4.4. Further perspectives on decision-making

In summary, we chose to focus here on understanding the putative striatal mechanisms underlying the observed differences in response selection between the control, Huntington's disease and BHC groups. This is a natural choice as the two disorders primarily affect the striatum, but it is likely that these experimental results will also provide fruitful ideas from other perspectives on decision-making and selection. We have focussed on response selection here, where once a perceptual decision is made that decision is mapped to the appropriate response. Recent theories have suggested that the striatum and the wider basal ganglia circuit also play a role in the perceptual component of decision-making, particularly in the process of accumulating evidence for each hypothesized perceptual alternative (Bogacz and Gurney, 2007; Lepora and Gurney, 2012; Ding and Gold, 2013).Ding and Gold (2010, 2012, 2013) have provided intriguing evidence for striatal activity encoding both response and evidence accumulation components in separate neural populations, and that this activity causally affects the final decision. Consequently, it is possible that the changes to striatum occurring in Huntington's disease and BHC could also influence the perceptual decision (here, whether the tone was short or long) as well as response selection. However, standard models of perceptual decision-making predict a speed-accuracy trade-off (Bogacz et al., 2006), whereby increased errors are the result of faster reaction times. Our data clearly show that both control and BHC groups increased both errors and reaction times on distractor trials: they thus present an interesting challenge to the models of perceptual decision-making.

Acknowledgements

We thank Kevin Gurney and Eleni Vasilaki for discussions, and Mehdi Khamassi for feedback on a draft of this paper. This work was supported by the Deutsche Forschungsgemeinschaft (DFG)

(grant number BE4045/10-1 to C.B.); the Agence Nationale de Recherche Programme Blanc (grant number ANR-2010-BLAN-0214-04 to M.D.H.); and a Medical Research Council (MRC) Senior non-Clinical Fellowship to M.D.H.

Appendix A. Supplementary material

Supplementary material associated with this article can be found, in the online version, at http://dx.doi.org/10.1016/j.nicl.2014.04.003.

References

Arning, L., Stock, A.-K., Kloster, E., Epplen, J.T., Beste, C., 2014. NPY2-receptor variation modulates iconic memory processes. European Neuropsychopharmacology. http://dx.doi.org/10.1016/j.euroneuro.2014.03.003.

Beiser, D.G., Hua, S.E., Houk, J.C., 1997. Network models of the basal ganglia. Current Opinion in Neurobiology 7, 185–90. http://dx.doi.org/10.1016/S0959-4388(97)80006-2, 9142759.

Beste, C., Saft, C., Güntürkün, O., Falkenstein, M., 2008. Increased cognitive functioning in symptomatic Huntington's disease as revealed by behavioral and event-related potential indices of auditory sensory memory and attention. Journal of Neuroscience: the Official Journal of the Society for Neuroscience 28, 11695–702. http://dx.doi.org/10.1523/JNEUROSCI.2659-08.2008, 18987205.

Beste, C., Schneider, D., Epplen, J.T., Arning, L., 2011. The functional BDNF Val66Met polymorphism affects functions of pre-attentive visual sensory memory processes. Neuropharmacology 60, 467–71. http://dx.doi.org/10.1016/j.neuropharm.2010.10.028, 21056046.

Beste, C., Stock, A.-K., Ness, V., Epplen, J.T., Arning, L., 2012. Differential effects of ADORA2A gene variations in pre-attentive visual sensory memory subprocesses. European Neuropsychopharmacology: the Journal of the European College of Neuropsychopharmacology 22, 555–61. http://dx.doi.org/10.1016/j.euroneuro.2011.12.004, 22240468.

Bogacz, R., Brown, E., Moehlis, J., Holmes, P., Cohen, J.D., 2006. The physics of optimal decision making: a formal analysis of models of performance in two-alternative forced-choice tasks. Psychological Review 113, 700–65. http://dx.doi.org/10.1037/0033-295X.113.4.700, 17014301.

Bogacz, R., Gurney, K., 2007. The basal ganglia and cortex implement optimal decision making between alternative actions. Neural Computation 19, 442–77. http://dx.doi.org/10.1162/neco.2007.19.2.442, 17206871.

Bracci, E., Panzeri, S., 2006. Excitatory GABAergic effects in striatal projection neurons. Journal of Neurophysiology 95, 1285–90, 16251264.

Chuhma, N., Tanaka, K.F., Hen, R., Rayport, S., 2011. Functional connectome of the striatal medium spiny neuron. Journal of Neuroscience: the Official Journal of the Society for Neuroscience 31, 1183–92. http://dx.doi.org/10.1523/JNEUROSCI.3833-10.2011, 21273403.

Crawford, J.R., Garthwaite, P.H., 2012. Single-case research in neuropsychology: a comparison of five forms of t-test for comparing a case to controls. Cortex; a Journal Devoted To the Study of the Nervous System and Behavior 48, 1009–16. http://dx.doi.org/10.1016/j.cortex.2011.06.021, 21843884.

Czubayko, U., Plenz, D., 2002. Fast synaptic transmission between striatal spiny projection neurons. Proceedings of the National Academy of Sciences of the United States of America 99, 15764–9. http://dx.doi.org/10.1073/pnas.242428599, 12438690.

Deng, Y.P., Albin, R.L., Penney, J.B., Young, A.B., Anderson, K.D., Reiner, A., 2004. Differential loss of striatal projection systems in Huntington's disease: a quantitative immunohistochemical study. Journal of Chemical Neuroanatomy 27, 143–64. http://dx.doi.org/10.1016/j.jchemneu.2004.02.005, 15183201.

Ding, L., Gold, J.I., 2010. Caudate encodes multiple computations for perceptual decisions. Journal of Neuroscience: the Official Journal of the Society for Neuroscience 30, 15747–59. http://dx.doi.org/10.1523/JNEUROSCI.2894-10.2010, 21106814.

Ding, L., Gold, J.I., 2012. Separate, causal roles of the caudate in saccadic choice and execution in a perceptual decision task. Neuron 75, 865–74. http://dx.doi.org/10.1016/j.neuron.2012.07.021, 22958826.

Ding, L., Gold, J.I., 2013. The basal ganglia's contributions to perceptual decision making. Neuron 79, 640–9. http://dx.doi.org/10.1016/j.neuron.2013.07.042, 23972593.

Douaud, G., Behrens, T.E., Poupon, C., Cointepas, Y., Jbabdi, S., Gaura, V. et al. 2009. In vivo evidence for the selective subcortical degeneration in Huntington's disease. NeuroImage 46, 958–66. http://dx.doi.org/10.1016/j.neuroimage.2009.03.044, 19332141.

Escera, C., Corral, M., 2007. Role of mismatch negativity and novelty-P3 in involuntary auditory attention. Journal of Psychophysiology 21, 251–64. http://dx.doi.org/10.1027/0269-8803.21.34.251.

Fan, M.M.Y., Raymond, L.A., 2007. N-Methyl-d-aspartate (NMDA) receptor function and excitotoxicity in Huntington's disease. Progress in Neurobiology 81, 272–93. http://dx.doi.org/10.1016/j.pneurobio.2006.11.003, 17188796.

Frank, M.J., Seeberger, L.C., O'Reilly, R.C., 2004. By carrot or by stick: cognitive reinforcement learning in parkinsonism. Science 306, 1940–3, 15528409.

Fukai, T., Tanaka, S., 1997. A simple neural network exhibiting selective activation of neuronal ensembles: from winner-take-all to winners-share-all. Neural Computation 9, 77–97. http://dx.doi.org/10.1162/neco.1997.9.1.77, 9117902.

Getzmann, S., Gajewski, P.D., Hengstler, J.G., Falkenstein, M., Beste, C., 2013. BDNF Val66Met polymorphism and goal-directed behavior in healthy elderly — evidence from auditory distraction. Neuroimage 64, 290–8. http://dx.doi.org/10.1016/j.neuroimage.2012.08.079, 22963854.

Gittis, A.H., Nelson, A.B., Thwin, M.T., Palop, J.J., Kreitzer, A.C., 2010. Distinct roles of GABAergic interneurons in the regulation of striatal output pathways. Journal of Neuroscience: the Official Journal of the Society for Neuroscience 30, 2223–34. http://dx.doi.org/10.1523/JNEUROSCI.4870-09.2010, 20147549.

Gras, D., Jonard, L., Roze, E., Chantot-Bastaraud, S., Koht, J., Motte, J. et al. 2012. Benign hereditary chorea: phenotype, prognosis, therapeutic outcome and long term follow-up in a large series with new mutations in the TITF1/NKX2-1 gene. Journal of Neurology, Neurosurgery & Psychiatry 83, 956–62. http://dx.doi.org/10.1136/jnnp-2012-302505.

Gurney, K., Prescott, T.J., Redgrave, P., 2001. A computational model of action selection in the basal ganglia. I. A new functional anatomy. Biological Cybernetics 84, 401–10. http://dx.doi.org/10.1007/PL00007984, 11417052.

Hikosaka, O., Sakamoto, M., Usui, S., 1989. Functional properties of monkey caudate neurons. I. Activities related to saccadic eye movements. Journal of Neurophysiology 61, 780–98, 2723720.

Hikosaka, O., Takikawa, Y., Kawagoe, R., 2000. Role of the basal ganglia in the control of purposive saccadic eye movements. Physiological Reviews 80, 953–78, 10893428.

Humphries, M.D., Lepora, N., Wood, R., Gurney, K., 2009. Capturing dopaminergic modulation and bimodal membrane behaviour of striatal medium spiny neurons in accurate, reduced models. Frontiers In Computational Neuroscience 3, 26, 20011223.

Humphries, M.D., Wood, R., Gurney, K., 2009. Dopamine-modulated dynamic cell assemblies generated by the GABAergic striatal microcircuit. Neural Networks: the Official Journal of the International Neural Network Society 22, 1174–88. http://dx.doi.org/10.1016/j.neunet.2009.07.018, 19646846.

Humphries, M.D., Wood, R., Gurney, K., 2010. Reconstructing the three-dimensional GABAergic microcircuit of the striatum. PLoS Computational Biology 6. http://dx.doi.org/10.1371/journal.pcbi.1001011, 21124867.

Inzelberg, R., Weinberger, M., Gak, E., 2011. Benign hereditary chorea: an update. Parkinsonism & Related Disorders 17, 301–7. http://dx.doi.org/10.1016/j.parkreldis.2011.01.002, 21292530.

Jaeger, D., Hitoshi, K., Wilson, C.J., 1994. Surround inhibition among projection neurons is weak or nonexistent in the rat neostriatum. Journal of Neurophysiology 72, 2555–8, 7884483.

Jahanshahi, M., Brown, R.G., Marsden, C.D., 1993. A comparative study of simple and choice reaction time in Parkinson's, Huntington's and cerebellar disease. Journal of Neurology, Neurosurgery & Psychiatry 56, 1169–77. http://dx.doi.org/10.1136/jnnp.56.11.1169.

Jahr, C.E., Stevens, C.F., 1990. Voltage dependence of NMDA-activated macroscopic conductances predicted by single-channel kinetics. Journal of Neuroscience: the Official Journal of the Society for Neuroscience 10, 3178–82, 1697902.

Javitt, D.C., Steinschneider, M., Schroeder, C.E., Arezzo, J.C., 1996. Role of cortical N-methyl-d-aspartate receptors in auditory sensory memory and mismatch negativity generation: implications for schizophrenia. Proceedings of the National Academy of Sciences of the United States of America 93, 11962–7. http://dx.doi.org/10.1073/pnas.93.21.11962, 8876245.

Kapur, N., Cole, J., Manly, T., Viskontas, I., Ninteman, A., Hasher, L. et al, 2013. Positive clinical neuroscience: explorations in positive neurology. Neuroscientist: a Review Journal Bringing Neurobiology, Neurology and Psychiatry 19, 354–69. http://dx.doi.org/10.1177/1073858412470976, 23286954.

Kleiner-Fisman, G., Calingasan, N.Y., Putt, M., Chen, J., Beal, M.F., Lang, A.E., 2005. Alterations of striatal neurons in benign hereditary chorea. Movement Disorders: Official Journal of the Movement Disorder Society 20, 1353–7. http://dx.doi.org/10.1002/mds.20577, 15986422.

Kleiner-Fisman, G., Lang, A.E., 2007. Benign hereditary chorea revisited: a journey to understanding. Movement Disorders: Official Journal of the Movement Disorder Society 22, 2297–305. http://dx.doi.org/10.1002/mds.21644, 17702033.

Koos, T., Tepper, J.M., Wilson, C.J., 2004. Comparison of IPSCs evoked by spiny and fast-spiking neurons in the neostriatum. Journal of Neuroscience: the Official Journal of the Society for Neuroscience 24, 7916–22. http://dx.doi.org/10.1523/JNEUROSCI.2163-04.2004, 15356204.

Kreitschmann-Andernahr, I., Rosburg, T., Demme, U., Gaser, E., Nowak, H., Sauer, H., 2001. Effect of ketamine on the neuromagnetic mismatch field in healthy humans. Brain Research. Cognitive Brain Research 12, 109–16, 11489614.

Lawrence, A.D., Sahakian, B.J., Robbins, T.W., 1998. Cognitive functions and corticostriatal circuits: insights from Huntington's disease. Trends in Cognitive Sciences 2, 379–88, 21227253.

Lawrence, A.D., Watkins, L.H., Sahakian, B.J., Hodges, J.R., Robbins, T.W., 2000. Visual object and visuospatial cognition in Huntington's disease: implications for information processing in corticostriatal circuits. Brain: a Journal of Neurology 123 (7), 1349–64. http://dx.doi.org/10.1093/brain/123.7.1349, 10869048.

Lepora, N.F., Gurney, K.N., 2012. The basal ganglia optimize decision making over general perceptual hypotheses. Neural Computation 24, 2924–45. http://dx.doi.org/10.1162/NECO_a_00360, 22920846.

Lester, R.A., Clements, J.D., Westbrook, G.L., Jahr, C.E., 1990. Channel kinetics determine the time course of NMDA receptor-mediated synaptic currents. Nature 346, 565–7. http://dx.doi.org/10.1038/346565a0, 1974037.

Mallet, N., Le, Moine C., Charpier, S., Gonon, F., 2005. Feedforward inhibition of projection neurons by fast-spiking GABA interneurons in the rat striatum in vivo. Journal of Neuroscience: the Official Journal of the Society for Neuroscience 25, 3857–69. http://dx.doi.org/10.1523/JNEUROSCI.5027-04.2005, 15829638.

Milnerwood, A.J., Gladding, C.M., Pouladi, M.A., Kaufman, A.M., Hines, R.M., Boyd, J.D. et al. 2010. Early increase in extrasynaptic NMDA receptor signaling and expression contributes to phenotype onset in Huntington's disease mice. Neuron 65, 178–90. http://dx.doi.org/10.1016/j.neuron.2010.01.008, 20152125.

Mink, J.W., 1996. The basal ganglia: Focused selection and inhibition of competing motor programs. Progress in Neurobiology 50, 381–425. http://dx.doi.org/10.1016/S0301-0082(96)00042-1, 9004351.

Mitchell, I.J., Cooper, A.J., Griffiths, M.R., 1999. The selective vulnerability of striatopallidal neurons. Progress in Neurobiology 59, 691–719. http://dx.doi.org/10.1016/S0301-0082(99)00019-2, 10845758.

Näätänen, R., Kujala, T., Escera, C., Baldeweg, T., Kreeqipuu, K., Carlson, S. et al, 2012. The mismatch negativity (MMN) — a unique window to disturbed central auditory processing in ageing and different clinical conditions. Clinical Neurophysiology: Official Journal of the International Federation of Clinical Neurophysiology 123, 424–58. http://dx.doi.org/10.1016/j.clinph.2011.09.020, 22169062.

Okamoto, S.I., Pouladi, M.A., Talantova, M., Yao, D., Xia, P., Ehrnhoefer, D.E. et al. 2009. Balance between synaptic versus extrasynaptic NMDA receptor activity influences inclusions and neurotoxicity of mutant huntingtin. Nature Medicine 15, 1407–13. http://dx.doi.org/10.1038/nm.2056, 19915593.

Planert, H., Szydlowski, S.N., Hjorth, J.J.J., Grillner, S., Silberberg, G., 2010. Dynamics of synaptic transmission between fast-spiking interneurons and striatal projection neurons of the direct and indirect pathways. Journal of Neuroscience: the Official Journal of the Society for Neuroscience 30, 3499–507. http://dx.doi.org/10.1523/JNEUROSCI.5139-09.2010, 20203210.

Plenz, D., 2003. When inhibition goes incognito: feedback interaction between spiny projection neurons in striatal function. Trends in Neurosciences 26, 436–43. http://dx.doi.org/10.1016/S0166-2236(03)00196-6, 12900175.

Prescott, T.J., Redgrave, P., Gurney, K., 1999. Layered control architectures in robots and vertebrates. Adaptive Behavior 7, 99–127. http://dx.doi.org/10.1177/105971239900700105.

Redgrave, P., Prescott, T.J., Gurney, K., 1999. The basal ganglia: a vertebrate solution to the selection problem? Neuroscience 89, 1009–23. http://dx.doi.org/10.1016/S0306-4522(98)00319-4, 10362291.

Saft, C., Schüttke, A., Beste, C., Andrich, J., Heindel, W., Pfleiderer, B., 2008. fMRI reveals altered auditory processing in manifest and premanifest Huntington's disease. Neuropsychologia 46, 1279–89. http://dx.doi.org/10.1016/j.neuropsychologia.2007.12.002, 18221758.

Schröger, E., Giard, M.H., Wolff, C., 2000. Auditory distraction: event-related potential and behavioral indices. Clinical Neurophysiology: Official Journal of the International Federation of Clinical Neurophysiology 111, 1450–60. http://dx.doi.org/10.1016/S1388-2457(00)00337-0, 10904227.

Schröger, E., Wolff, C., 1998. Attentional orienting and reorienting is indicated by human event-related brain potentials. Neuroreport 9, 3355–8. http://dx.doi.org/10.1097/00001756-199810260-00003, 9855279.

Shiner, T., Seymour, B., Wunderlich, K., Hill, C., Bhatia, K.P., Dayan, P. et al, 2012. Dopamine and performance in a reinforcement learning task: evidence from Parkinson's disease. Brain: a Journal of Neurology 135, 1871–83. http://dx.doi.org/10.1093/brain/aws083, 22508958.

Stout, J.C., Wylie, S.A., Simone, P.M., Siemers, E.R., 2001. Influence of competing distractors on response selection in Huntington's disease and Parkinson's disease. Cognitve Neuropsychology 18, 643–53. http://dx.doi.org/10.1080/02643290126376l0.1080/026432901430010015.

Sussel, L., Marin, O., Kimura, S., Rubenstein, J.L., 1999. Loss of Nkx2.1 homeobox gene function results in a ventral to dorsal molecular respecification within the basal telencephalon: evidence for a transformation of the pallidum into the striatum. Development (Cambridge, England) 126, 3359–70, 10393115.

Taverna, S., van Dongen, Y.C., Groenewegen, H.J., Pennartz, C.M., 2004. Direct physiological evidence for synaptic connectivity between medium-sized spiny neurons in rat nucleus accumbens in situ. Journal of Neurophysiology 91, 1111–21, 14573550.

Tepper, J.M., Koos, T., Wilson, C.J., 2004. GABAergic microcircuits in the neostriatum. Trends in Neurosciences 27, 662–9. http://dx.doi.org/10.1016/j.tins.2004.08.007, 15474166.

Tunstall, M.J., Oorschot, D.E., Kean, A., Wickens, J.R., 2002. Inhibitory interactions between spiny projection neurons in the rat striatum. Journal of Neurophysiology 88, 1263–9, 12205147.

Umbricht, D., Koller, R., Vollenweider, F.X., Schmid, L., 2002. Mismatch negativity predicts psychotic experiences induced by NMDA receptor antagonist in healthy volunteers. Biological Psychiatry 51, 400–6. http://dx.doi.org/10.1016/S0006-3223(01)01242-2, 11904134.

Yim, M.Y., Aertsen, A., Kumar, A., 2011. Significance of input correlations in striatal function. PLoS Computational Biology 7. http://dx.doi.org/10.1371/journal.pcbi.1002254, 22125480.

Yoshida, Y., Nunomura, J., Shimohata, T., Nanjo, H., Miyata, H., 2012. Benign hereditary chorea 2: Pathological findings in an autopsy case. Neuropathology: Official Journal of the Japanese Society of Neuropathology 32, 557–65. http://dx.doi.org/10.1111/j.1440-1789.2011.01288.x, 22239265.

Znamenskiy, P., Zador, A.M., 2013. Corticostriatal neurons in auditory cortex drive decisions during auditory discrimination. Nature 497, 482–5. http://dx.doi.org/10.1038/nature12077, 23636333.

Tabrizi, S.J., Langbehn, D.R., Leavitt, B.R., Roos, R.A., Durr, A., Craufurd, D. et al, 2009. Biological and clinical manifestations of Huntington's disease in the longitudinal TRACK-HD study: cross-sectional analysis of baseline data. Lancet Neurology 8, 791–801.

Kujala, T., Tervaniemi, M., Schröger, E., 2007. The mismatch negativity in cognitive and clinical neuroscience: theoretical and methodological considerations. Biological Psychology 74, 1–19.